



# 1 International airport emissions and their impact on local air 2 quality: Chemical speciation of ambient aerosols at Madrid- 3 Barajas Airport during AVIATOR Campaign

4 Saleh Alzahrani<sup>1</sup>, Doğuşhan Kılıç<sup>1,2</sup>, Michael Flynn<sup>1</sup>, Paul I. Williams<sup>1,2</sup> and James Allan<sup>1,2</sup>

5 <sup>1</sup>Department of Earth and Environmental Sciences, University of Manchester, Manchester, UK

6 <sup>2</sup>National Centre for Atmospheric Science, University of Manchester, Manchester, UK

7  
8  
9  
10  
11 Correspondence to: Saleh Alzahrani ([Saleh.alzahrani@manchester.ac.uk](mailto:Saleh.alzahrani@manchester.ac.uk))

12  
13  
14 **Abstract.** Madrid-Barajas International Airport (MAD), located in Spanish Capital Madrid, is the fourth-busiest  
15 airport in Europe. As part of the AVIATOR campaign, chemical composition of particulate matter and other key  
16 pollutants were measured at the airport perimeter during October 2021, to assess the impact of airport emissions  
17 on local air quality. A high-fidelity ambient instrumentation system was deployed at Madrid Airport to measure:  
18 composition of ambient aerosol and concentrations of black carbon (*e*BC), carbon dioxide (CO<sub>2</sub>), carbon monoxide  
19 (CO), nitrogen dioxide (NO<sub>x</sub>), sulphur dioxide (SO<sub>2</sub>), particulate matter (PM<sub>2.5</sub>, PM<sub>10</sub>), total hydrocarbon (THC),  
20 and total particle number. The average concentration for the entire campaign of *e*BC, NO<sub>x</sub>, SO<sub>2</sub>, PM<sub>2.5</sub>, PM<sub>10</sub>, CO  
21 and THC at the airport were, 1.07 (µg/m<sup>3</sup>), 22.7 (µg/m<sup>3</sup>), 4.10 (µg/m<sup>3</sup>), 9.35 (µg/m<sup>3</sup>), 16.43 (µg/m<sup>3</sup>), 0.23 (mg/m<sup>3</sup>)  
22 and 2.30 (mg/m<sup>3</sup>) respectively. The source apportionment analysis of the non-refractory organic aerosol (OA)  
23 using positive matrix factorisation (PMF) allowed us to discriminate between different sources of pollution,  
24 namely: Semi Volatile Oxygenated Organic Aerosol (SV-OOA), Alkane Organic Aerosol (AlkOA), and More  
25 Oxidised Oxygenated Organic Aerosol (MO-OOA) source. The results showed that SVOOA and MO-OOA  
26 accounts for more than 80% of the total organic particle mass that was measured near runway at the airport. Trace  
27 gases correlate better with AlkOA factor more than SVOOA and MO-OOA which indicate that AlkOA is mainly  
28 related to the primary emissions of combustion. Bivariate polar plots were used for the source identification.  
29 Significantly higher concentrations of the obtained factors were observed at low wind speeds < 3m/s from the  
30 southwest where two of runways, as well as all terminals are located. Higher SO<sub>2</sub>/NO<sub>x</sub> and CO/*e*BC ratios were  
31 observed when the winds originating from the northeast where the 18L/36R runways are located. This is attributed  
32 to the aircraft influence and the lack of a local road source in the northeast area.

## 33 34 35 1. Introduction

36  
37 Several studies have linked particulate matter (PM) to a range of harmful health effects, including respiratory  
38 and cardiovascular ailments ([Boldo et al., 2006](#); [Li et al., 2003a](#); [Pope and Dockery, 2006](#); [Schwarze et al. et al., 2006](#)). In recent years, a number of researchers have found an association between aviation emissions and potential  
39 adverse human health impacts. These emissions can lead to immune system malfunction, various pathologies, the  
40 development of cancer, and premature death. Hence, it is increasingly recognised as a serious, worldwide public  
41 health concern ([Yim et al., 2013](#); [He et al., 2018](#); [Jonsdottir et al., 2019](#)).

42 A few studies have reported that air pollutants emitted from large airports can play a vital role in worsening  
43 the regional air quality ([Rissman et al., 2013](#); [Hudda and Fruin, 2016](#)). [Hu et al., \(2009\)](#) and [Westerdahl et al., \(2008\)](#) measured high ambient PM concentrations downwind of Los Angeles International Airport (LAX) and  
44 Santa Monica Airport (SMA) in California. A decline in the ambient air quality was observed over distances of  
45 up to 18 km downwind from international airports owing to gas turbine-emitted PM ([Hudda et al., 2014](#); [Hudda  
46 and Fruin, 2016](#)). Airports' contribution to primary and secondary inhalable and fine particulate matter (PM<sub>10</sub> and  
47 PM<sub>2.5</sub>, mass of particles with aerodynamic diameters <10 µm and <2.5 µm, respectively) making them  
48 determinants of the air quality in cities and a significant issue for the local air quality management. To date, several  
49 questions still remain to be answered regarding the chemical composition of aircraft plumes, and the health risks  
50 associated with the exposure to the pollutants originating from airports in neighbouring communities. Responding  
51 to the growing concern about the risk of exposure to airport pollutants, studies have been conducted to gain a  
52 better understanding of airport emissions and their possible effects on local and regional air quality. Thus far,  
53 aircraft engines are considered to be one of the major sources of both gaseous and particulate pollutants at the  
54 airport ([Masiol and Harrison, 2014](#)). Various campaigns have reported both physical and chemical properties of  
55  
56



57 particulate and gaseous emissions ([Kinsey, 2009](#); [Kinsey et al., 2010, 2011](#); [Mazaheri et al., 2011](#); [Hudda et al.,](#)  
58 [2016](#)).

59 Aviation fuel Jet A1 is the most common type of fuel that is used in civil aviation. It's a complex mixture of  
60 aliphatic hydrocarbons, characterized by a mean C/H ratio of ~ 0.52 (with an average empirical molecular formula  
61 of C<sub>12</sub>H<sub>23</sub>) ([Lee et al., 2010](#)). Several fuel combustion sources are present at airports, including aircraft operation  
62 and diesel ground transport that services the airport and brings in passengers for traveling. Fuel combustion likely  
63 caused maximum particle counts in 10 - 20 nm range based on the particle size distribution analysis ([Zhu et al.,](#)  
64 [2011](#)). There are also other sources of airport-related PM emissions that contribute to air pollution at the local  
65 scale. Particulate pollution (38% of PM<sub>10</sub> with a mean level of 48 µg/m<sup>3</sup>) at airports can periodically originate  
66 from the construction activities for terminal maintenance and construction ([Amato et al., 2010](#)). Particles emitted  
67 by commercial aircraft can be divided into two main groups: non-volatile and volatile PM. Non-volatile PM  
68 (nvPM) is usually formed during the (incomplete) combustion process and then emitted from the aircraft  
69 combustion chamber. It consists mostly of carbonaceous substances such as soot, dust, and trace metals ([Yu et](#)  
70 [al., 2019](#)). nvPM has the physical property of being resistant to high temperatures and pressure. On the other hand,  
71 volatile PM is formed through gas to particle conversion process, primarily by sulphur and organic compounds,  
72 which exist in the exhaust gas downstream of the engine after emission. Sulphuric compounds are formed as a  
73 result of sulphur in fuel, whereas organic particles are formed as combustion products, and from fuel and oil  
74 vapours ([ICAO, 2016](#); [Smith et al., 2022](#)). Aircraft and ground unit emissions have been documented in prior  
75 research ([Masiol and Harrison, 2014](#)), yet there is still a gap in knowledge about airport-related PM emissions in  
76 terms of (i) apportioning PM to individual sources at airports, (ii) specifying their chemical composition, and (iii)  
77 the wider impacts of PM on local communities. This study set out to obtain data that will help to address these  
78 research gaps by providing further in-depth information on particle composition measurements and key pollutants  
79 observed within an airport environment, through characterizing organic volatile PM emissions aiming to assess  
80 the effect of aviation emissions on the local air quality. Here we focus on Adolfo Suárez Madrid-Barajas Airport  
81 in Madrid. As part of the AVIATOR Project (Assessing aViation emission Impact on local Air quality at airports:  
82 TOwards Regulation), several experiments were conducted at the Madrid-Barajas Airport, for monitoring the  
83 chemical properties of sub-micron particles. Source apportionment analysis was performed based on the particle  
84 data collected via high resolution mass spectrometry and this analysis allowed us to discriminate between different  
85 sources of pollution at the airport microenvironment. These findings will serve as the foundation for additional  
86 comprehensive research, such as toxicological and health effect studies of PM originating from aviation activities.  
87

## 88 2. Methods

### 89 2.1. Description of the sampling location

90 Adolfo Suárez Madrid-Barajas Airport is the main international airport, located within the municipal limits of  
91 Madrid, 13 km northeast of Madrid's city centre. It is the fourth-busiest airport in Europe based on passenger  
92 volume ([Eurostat Database, 2021](#)). In 2019, 62 million travellers used Madrid-Barajas and nearly half a million  
93 aircraft movements have been recorded, making it the largest and busiest airport in the country. In 2021, nearly  
94 one-third of the previous number travelled through Madrid Airport because of the COVID-19 pandemic. The  
95 airport has five passenger terminals named T1, T2, T3, T4, and T4S. Barajas Airport has four runways: two on  
96 the north-south axis and parallel to each other 18L/36R - 18R/36L and two on the northwest-southeast axis  
97 14L/32R - 14R/32L. The runways enable takeoff and landing simultaneously at the airport, allowing 120  
98 operations per hour (one takeoff or landing every 30 seconds). The sampling location was chosen in concert with  
99 AENA, the owner and operator of the Barajas Airport to facilitate the provision of power and access for servicing.  
100 Focusing on the temporal and spatial monitoring of the key pollutants, the site was positioned between runways  
101 36L and 36R to sample the airport emissions from an optimal sampling point for aviation activities (Fig.1).  
102  
103

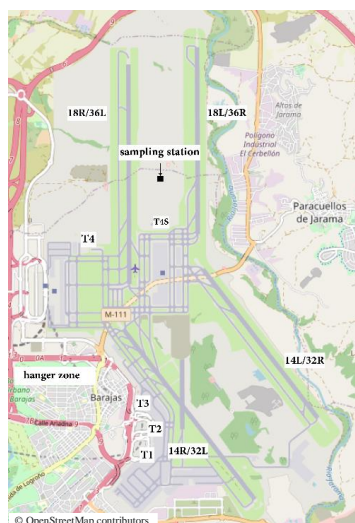


**Figure 1. Locations of runways, terminals, and sampling site at Adolfo Suárez Madrid-Barajas Airport. Measurements were performed between October 8, 2021 and October 23, 2021. (Adapted from: <https://www.openstreetmap.org>)**

104  
105  
106  
107  
108  
109  
110  
111  
112  
113  
114  
115  
116  
117  
118  
119  
120  
121  
122  
123  
124  
125  
126  
127  
128  
129  
130  
131  
132  
133  
134  
135  
136  
137  
138  
139  
140  
141  
142  
143

## 2.2. Sampling and instrumentation

The autumn campaign of AVIATOR took place in October 2021. Sampling was conducted continuously, starting at 12:00 pm on October 8, 2021 and ending at 20:00 pm on October 23, 2021. An ambient instrumentation system with specific reference to PM was deployed at Madrid Airport to better characterise air quality at the airport microenvironment. The measurement equipment of the system includes an Aerodyne High-Resolution Time-of-Flight Aerosol Mass Spectrometer (AMS) for the chemical speciation of the particles. AMS measures concentration and chemical composition of non-refractory aerosols online. AMS provided high-resolution measurements of primary and secondary organic aerosol and inorganic aerosol including sulphates, nitrates, and ammonium, from approximately 60 nm to 600 nm with 100 % transmission, extending to smaller and larger sizes with reduced transmission (Canagaratna *et al.*, 2007). In addition to daily standard AMS flow, baseline and single ion calibrations, an ammonium nitrate solution was atomised to calibrate the AMS (for size-dependent ionisation efficiency). The analysis of the chemical characteristics of aircraft PM using an AMS have been described elsewhere in detail (Yu *et al.*, 2010; Anderson *et al.*, 2011; Smith *et al.*, 2022).

Equivalent black carbon mass concentration (*eBC*) based on aerosol optical absorption was monitored using the Multi-Angle Absorption Photometer (MAAP) during this campaign. The MAAP operates at 670nm wavelength, has a 10s-time response with a flow rate of 8 litre/min, for unattended long-term monitoring of carbonaceous particulate emissions from combustion sources (Petzold and Schonlinner, 2004). MAAP has been used for the monitoring of black carbon emission from aviation (Herndon *et al.*, 2008; Timko *et al.*, 2014). The instrument was set up to measure average *eBC* concentrations with one-minute intervals. By using a condensation particle counter (CPC), TSI model 3750 ( $D_{50} \approx 7\text{nm}$ ), total particle number concentration was measured real-time to capture temporal variability in particle number concentrations with a measurement range of up to 100,000 particles/cm<sup>3</sup> and a time resolution of one second. Ambient CO<sub>2</sub> concentration near runways were also measured by a LI-COR CO<sub>2</sub> Trace Gas Analysers at 1-sec intervals. In addition, meteorological parameters (temperature, pressure, relative humidity, wind speed, and direction) were measured at the site with the instrumentation system. The system was co-located with AENA (REDAIR) fixed monitoring site to provide additional spatially resolved data. The REDAIR station monitors the concentration of sulphur dioxide (SO<sub>2</sub>), nitrogen dioxide (NO<sub>x</sub>), carbon monoxide (CO), ozone (O<sub>3</sub>), suspended particles PM (including PM<sub>2.5</sub>, PM<sub>10</sub>), and total hydrocarbon (THC) with a time resolution of 30 minutes.



### 144 2.3. Data analysis

145

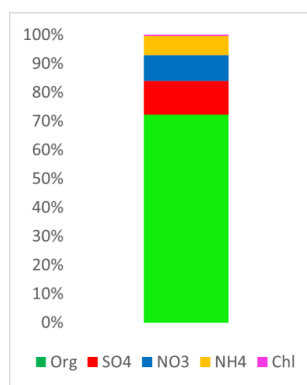
146 AMS was operating in Mass Spectrum (MS) mode to identify chemical species present in the aerosol ensemble  
 147 and quantify the overall mass loading. AMS data were analysed using the data analysis toolkit TOF-AMS  
 148 SQUIRREL v1.65B supplied by Igor Pro (WaveMetrics, Inc.). Source apportionment analysis is an approach to  
 149 investigate the relative contributions of various source pollutants in a sample. Using the updated graphical  
 150 interface source finder (SoFi) to carry out non-refractory OA source apportionment analysis with using PMF  
 151 model implemented through the multilinear engine tool (ME-2) (Canonaco *et al.*, 2013). The software Source  
 152 Finder (SoFi) run under IGOR 6.37 was used to deconvolve organic aerosol emissions via the Positive Matrix  
 153 Factorization (PMF) model. PMF model implemented through the multilinear engine version 2 (ME-2)  
 154 factorisation tool was used to determine the number of factors (sources). ME-2 is a multivariate solver that uses  
 155 the same mathematical/statistical method as PMF to evaluate solutions (Paatero, 1999). ME-2 equations are  
 156 designed for analysing and calculating the relative contributions of various source pollutants by measuring their  
 157 concentration at receptor locations (Paatero and Tapper, 1994). The PMF model collects many variables and filters  
 158 them into two types (i) source types which can be determined by matching these sources to measured reference  
 159 profiles, and (ii) source contributions, used to quantify the amount of contribution from each source to a sample.  
 160 PMF inputs were restricted to only non-negative concentrations since no sample can have a negative source  
 161 contribution. A step-by-step approach was used to select the number of solutions (factors). The method used by  
 162 Reyes *et al.* (2016) and Smith *et al.* (2022) was used to determine the optimal solution. This approach initially  
 163 began with a two-factor model and then increased to a maximum of five factors. PMF analysis was performed  
 164 with seed runs and different FPEAK values (ranging from -1 to 1 with steps of 0.1) to better separate organic  
 165 aerosol sources. During the analysis, it has been noted that factor four seems to consistently correlate with factor  
 166 five with identical time series and similarities in mass spectra. The difficult separation has been found previously  
 167 in the case of well-mixed pollutants due to low temperatures and wind speed (Reyes *et al.*, 2018). Greater stability  
 168 was found when analysing 3-factor solutions with different FPEAK values. During the analysis, seed runs and  
 169 PMF with FPEAK solutions show no significant variation on the  $Q / Q_{exp}$  with a value close to 1. This is  
 170 reasonable given that PMF determines the solution by minimising this value. (Reyes *et al.*, 2016). The  
 171 factorisation strategy has been completely successful to separate three different sources with distinct mass spectra  
 172 and different time series. Consequently, 3-factor solutions were the optimal number of sources because of their  
 173 best performance in terms of lowest residuals and  $Q/Q_{exp}$  values which is close to 1.

174

## 175 3. Results and Discussion

### 176 3.1 Variations of organic, inorganic, and oil emissions

177



178

179 **Figure 2. The bar chart shows aerosol fractions where organic and sulphate species account for more than 80% of the**  
 180 **total aerosol mass.**

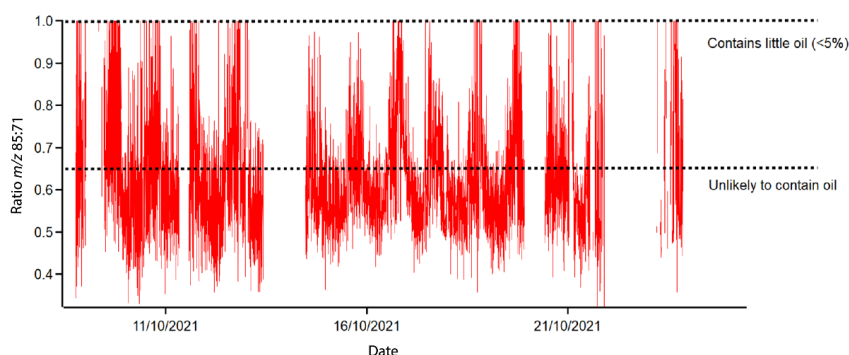
181

182

183 Mass concentrations of organic and inorganic aerosols was  $9.6 \mu\text{g}/\text{m}^3$  on average for the entire campaign. Organic  
 184 aerosols, with a significantly high fraction compared to the nearest sulphate with 15 % accounts for about 70% of  
 185 the total aerosols measured by AMS. Figure 2 shows aerosol fractions where organics account for about 70% of  
 186 the aerosol. The PMF analysis in this paper mainly focuses on the composition of the organic mass concentration.  
 187 Lubrication oil has been detected in ambient air near runways, and it may further add to the total organic PM  
 188 emissions due to aircraft engine operations (Timko *et al.*, 2010b; Yu *et al.*, 2010; Ungeheuer *et al.*, 2022). Aircraft  
 189 plume measurements indicated that oil was found to contribute 5% to 100% (Yu *et al.*, 2012). The  $m/z$  85 signal  
 190 is a well-known oil signal in the AMS mass spectrum. Ratio of  $m/z$  85:71 is used as a marker for oil (Fig. 3). The



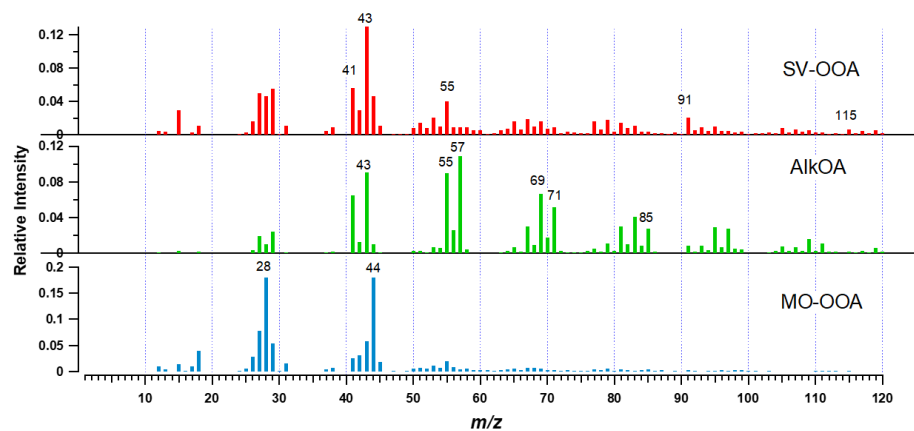
191 ratio of 0.66 was used as a benchmark for oil contribution (Yu *et al.*, 2012). A value less than 0.66 can be  
 192 considered oil-free organic PM and conversely, any value larger than 0.66 indicates the presence of lubrication  
 193 oil. However, based on the AMS measurements during AVIATOR autumn campaign, lubrication oil accounted  
 194 only up to 5% of the total aerosol mass, which is significantly less compared to the measurements of Yu *et al.*  
 195 (2012). There are three probable explanations on the deficiency of AMS to detect oil precursors: (i) the oil particles  
 196 are too small in diameter for AMS to detect, (ii) complete pyrolysis of the oil in the engine combustion zone  
 197 forming carbon monoxide (CO) and carbon dioxide (CO<sub>2</sub>) (Smith *et al.*, 2022) or (iii) oil particles contribute to  
 198 an insignificant amount (by mass) of organic mass in engine exhaust therefore are not detected. Since PMF  
 199 analysis is based on the organic masses measured via AMS, lubrication oil is not identified as a determinant and  
 200 there is no oil organic mass profile reported in previous studies and here (Ulbrich *et al.*, 2009). PMF has been  
 201 proven inefficient at detecting such levels (Ulbrich *et al.*, 2009), therefore, oil contribution to the organic mass  
 202 can be under-represented in this study.  
 203



204  
 205  
 206  
 207  
 208  
 209  
 210  
 211  
 212  
 213

**Figure 3. Temporal variability of lubrication oil fraction in total aerosol mass obtained from AMS measurements. The ratio of  $m/z$  85/71 was used as the mass marker to identify lubrication oil. The analysis showed that no oil or very little (<5%) oil fraction was detected.**

### 3.2 PMF Analysis



214  
 215  
 216  
 217  
 218  
 219  
 220  
 221

**Figure 4. The mass spectral fingerprint of the three factors from the PMF solutions. Semi-Volatile Oxygenated Organic Aerosol (SV-OOA), Alkane Organic Aerosol (AlkOA), and More Oxidised Oxygenated Organic Aerosol (MO-OOA), which can be indicative of secondary aerosols. Selected mass markers with a relative intensity higher than 0.01 are numbered.**



222 The PMF analysis in this study aims to provide relative contribution of the sources of aerosols near runway. In  
223 addition to determining the diurnal pattern of the obtained factors during the autumn campaign, PMF solutions  
224 were used to investigate how meteorology affects airborne particulate pollution. During AVIATOR Autumn  
225 Campaign at Madrid-Barajas International Airport three sources were identified via PMF (Fig. 4 shows the results  
226 of the PMF analysis, the mass spectral fingerprint). The first factor in Fig. 4 shows the presence of an aromatic  
227 marker at  $m/z$  115, a marker used for identifying indene ( $C_9H_8$ ) ion in an earlier studies focusing on aviation  
228 emissions (Timko *et al.*, 2014). The Semi-Volatile Oxygenated Organic Aerosol (SV-OOA) is associated with  
229 aromatic fragments at  $m/z$  77, 91, 105, 115. It presents a high relative intensity (0.13) at  $m/z$  43 (characteristic of  
230 SVOOA) and a lower relative intensity ( $<0.04$ ) at  $m/z$  91 which is related to toluene ion ( $C_7H_7$ ) (Smith *et al.*,  
231 2022). Due to the strong correlation ( $R = 0.91$ ) and similarity in the mass spectra of SV-OOA in this study and  
232 the SV-OOA in Smith *et al.*, 2022, we consider that SV-OOA factor in our analysis potentially represent fresh  
233 secondary organic aerosols (SOA). This factor has high diurnal variation (varying with ambient temperature) since  
234 ambient temperature is a significant determinant of SV-OOA factor (Reves *et al.*, 2016). Concentrations of SV-  
235 OOA is lowest at noon when the ambient temperature is highest (Fig. 5). In a previous PMF analysis of organic  
236 PM emitted by aircraft indicated that aromatic factor was strongly present in the organic PM with elevated signals  
237 at  $m/z$  77, 91, 105, 115, 128 (Timko *et al.*, 2014). The aromatic factor determined by Timko *et al.*, 2014 was found  
238 to dominate the organic PM emissions from turbo-jet engine at low-thrust engine settings. The factor was linked  
239 with the products of incomplete combustion and had a high variability, varying with the engine power settings  
240 (the sum of signals in the factor decreased with the increasing engine power).

241 The second factor, identified based on the PMF analysis of Madrid airport sample, is Alkane Organic Aerosol  
242 (AlkOA) factor. It is related to unburnt fuel and incomplete combustion emission with high relative intensities at  
243  $m/z$  43, 57, and 85 (typically decane,  $C_{10}H_{22}$ , which is an alkane found in jet fuel). Given that mass spectral  
244 fingerprint of decane is similar to the other aliphatic hydrocarbons (*e.g.*, long-chain alkanes) found in Jet A1 fuel  
245 (Yu *et al.*, 2012; Smith *et al.*, 2022). AlkOA factor referred here as a marker to identify emissions originating  
246 from unburnt fuel/incomplete fuel combustion products. Previously, primary aliphatic factor was found in PMF  
247 analysis by Timko *et al.* (2014) and was attributed based on  $m/z$  ratios such as 41/43, 55/57, 69/71, 83/85. Each  
248 of these masses correspond to an alkane. Aliphatic #1 was strongly correlated with black carbon soot emissions  
249 for the high-power conditions. The strong association of aliphatic #1 with soot emissions indicated that they have  
250 similar combustion sources. It was concluded that aliphatic #1 derived from combustion related sources and can  
251 potentially contain significant unburnt jet fuel. Further, there is a strong positive linear correlation between the  
252 determined AlkOA and decane factor from NIST webbook ( $R = 0.83$ ) NIST Mass Spectrometry Data Center,  
253 1990), and between the determined AlkOA factor in this study and the AlkOA factor reported by (Smith *et al.*,  
254 2022) ( $R = 0.93$ ). The positive linear correlation among these three factors is indicative of similar primary  
255 pollutants derived from fuel vapours or incomplete combustion products originating from jet fuel. Results are  
256 consistent with previous findings of another study (Smith *et al.*, 2022). The third factor More Oxidised  
257 Oxygenated Organic Aerosol (MO-OOA) has a spectral fingerprint consists of more oxidised ions (compared to  
258 SV-OOA and AlkOA) indicating a secondary aerosol fraction in the sample. MO-OOA is identified by its  
259 characteristic high relative intensities ( $>0.18$ ) at  $m/z$  29 and 44. Given that MO-OOA has the highest  $f_{44/43}$  ratio  
260 among the three factors, it is expected to be the most oxygenated (in chemical content) factor. Being more oxidised  
261 potentially makes MO-OOA less volatile than SV-OOA (Jimenez *et al.*, 2009; Smith *et al.*, 2022). Other sources  
262 may have been included in one or both factor solutions, consequently, this does not rule out the possibility of their  
263 existence.

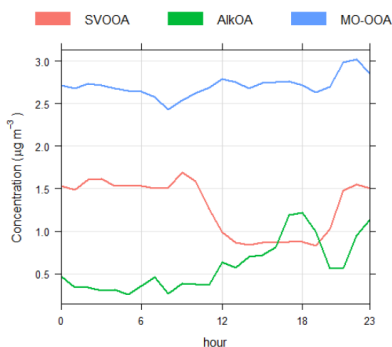
264

### 265 3.3 The temporal distribution of factors and correlation with trace gases

266

267





268  
269  
270  
271

**Figure 5. Diurnal pattern of the solved factors from October 8, 2021 to October 23, 2021. Compared to SV-OOA and AlkOA; MO-OOA has the smallest variation in its diurnal pattern.**

272  
273  
274  
275  
276  
277  
278  
279  
280  
281  
282  
283  
284  
285  
286  
287  
288  
289  
290  
291  
292  
293  
294  
295  
296  
297  
298  
299  
300  
301  
302  
303

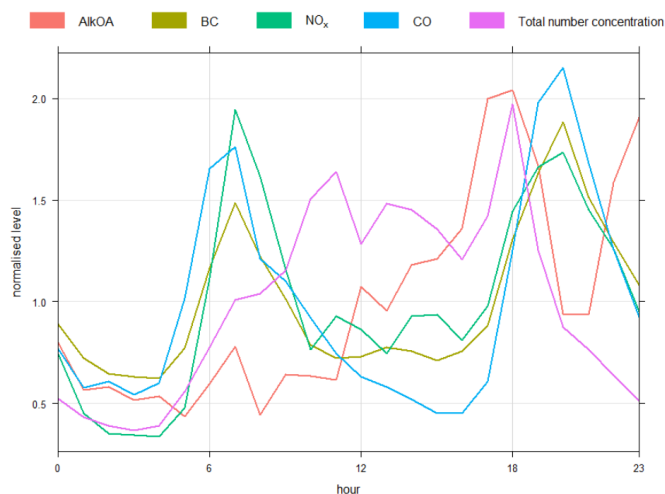
Average hourly concentrations of the PMF determined factors were calculated to monitor the diurnal variation of the source contributions. The variation of the AlkOA concentration during the day mostly associated with aircraft emissions (Fig. 5). The concentration of AlkOA factor is relatively higher in the afternoon compared to the morning and midday. This diurnal AlkOA pattern is similar to the diurnal flight activity and indicates that the AlkOA increase starting at noon is related to the primary particles emitted by aircraft. This source is previously reported as the main determinant of the air quality in the vicinity of the airport (Masiol and Harrison, 2014). Ambient temperature is the major determinant of the SVOOA. SVOOA has the lowest concentrations in the afternoon and increases in the evening until noon. Decreasing ambient temperature causing SVOOA to partition to the particle phase is the probable cause of the increase in the evenings. Unlike other factors, MO-OOA has no significant diurnal variation. This gives an indication of the formation of aged secondary organic aerosols which is often due to atmospheric transport (Zhang *et al.*, 2007). AlkOA was moderately correlated with *e*BC, NO<sub>x</sub>, SO<sub>2</sub>, and CO at Madrid-Barajas Airport as the linear correlation coefficients are given in Table 1 (R=0.56, R =0.52, R =0.53, and R =0.52). In contrast, the correlation of these trace gases with the SVOOA and MO-OOA is lower compared to AlkOA since R values ranging from 0.2 to 0.5 (Table 1). The reason that AlkOA has a slightly higher correlation (R > 0.5) with BC, NO<sub>x</sub>, SO<sub>2</sub> and CO compared to SVOOA and MO-OOA, AlkOA is considered to be a primary pollutant (directly emitted by the source) whereas SVOOA and MO-OOA are theoretically formed through condensation and/coagulation of primary pollutants.

Further, diurnal patterns of BC, NO<sub>x</sub>, SO<sub>2</sub> and CO can be significantly affected by meteorological conditions (*e.g.*, wind speed, temperature) (Carslaw *et al.*, 2006; Reyes *et al.*, 2018) which explains their moderate correlation with AlkOA, R values ranging from 0.52 to 0.56 (Table 1). AlkOA and trace gases were normalized to compare their diurnal patterns. Figure 6 shows diurnal patterns of *e*BC, NO<sub>x</sub>, CO, and particle number concentration. Their diurnal pattern is mostly similar, there are very pronounced increases in concentrations for *e*BC, NO<sub>x</sub>, and CO during am and pm rush hours. Early morning AlkOA concentration is significantly lower compared to *e*BC, NO<sub>x</sub>, and CO. This could be due to the lower emissions from decreased aircraft activities in early mornings. Early morning increase in trace gases and *e*BC may be due to other airport activities. These other activities potentially include emissions from vehicles for ground services and ground service equipment at the airport (Masiol and Harrison, 2014). The total number concentration had a temporal pattern similar to AlkOA. Throughout the day, AlkOA and trace gases' temporal profiles were also similar. The similarity in temporal profiles indicates similar source origins which can be associated temporally with aircraft activity.

**Table 1 Results of linear regression analysis between obtained factors (SVOOA, AlkOA, and MO-OOA) and external tracers**

|        | <i>e</i> BC (µg/m <sup>3</sup> ) | NO <sub>x</sub> (µg/m <sup>3</sup> ) | SO <sub>2</sub> (µg/m <sup>3</sup> ) | CO (mg/m <sup>3</sup> ) | THC (mg/m <sup>3</sup> ) | PM2.5 (µg/m <sup>3</sup> ) | Tot No. conc (particles/cm <sup>3</sup> ) | CO2 (ppm) |
|--------|----------------------------------|--------------------------------------|--------------------------------------|-------------------------|--------------------------|----------------------------|---|-----------|
| SVOOA  | 0.49                             | 0.28                                 | 0.21                                 | 0.32                    | 0.63                     | 0.36                       | -0.08                                     | 0.24      |
| AlkOA  | 0.56                             | 0.52                                 | 0.53                                 | 0.52                    | 0.35                     | 0.66                       | 0.4                                       | 0.35      |
| MO-OOA | 0.48                             | 0.36                                 | 0.26                                 | 0.45                    | 0.41                     | 0.55                       | 0.1                                       | 0.22      |

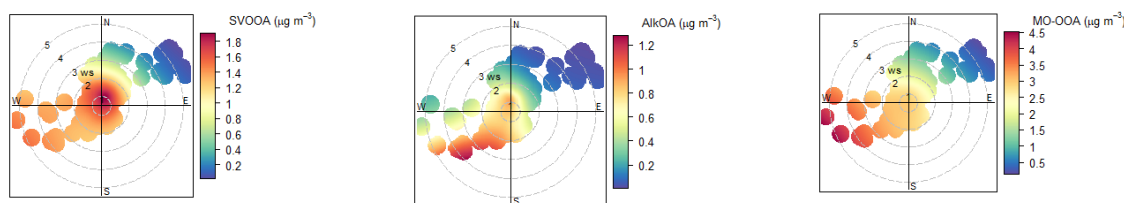
304  
305  
306  
307



308  
309  
310  
311  
312  
313  
314

**Figure 6. The diurnal cycle of AlkOA compared to eBC, NO<sub>x</sub>, CO, and total number concentration. In this plot, the concentrations are normalised with the objective of comparing the patterns of different pollutants using the same scale.**

### 3.4 Spatial analysis



315  
316  
317  
318  
319  
320  
321  
322  
323  
324  
325  
326  
327  
328  
329  
330  
331  
332  
333  
334  
335  
336  
337

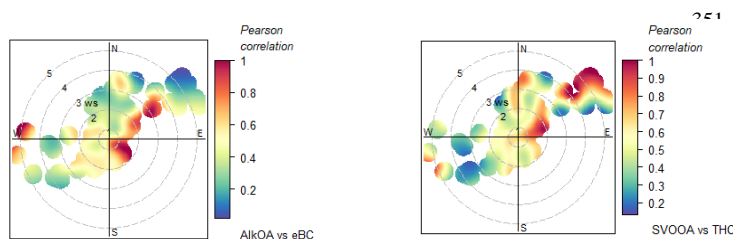
**Figure 7. Bivariate polar plots for SVOOA, AlkOA, and MO-OOA ( $\mu\text{g}/\text{m}^3$ ). The highest concentrations were measured when the winds were originated from the west and southwest. Runways 18R/36L and 14R/32L located at western and eastern sides of the measurement station and the hanger zone with terminals T1, T2, T3, T4, and TS4 were located at the south and southwest of the measurement site (Fig. 1).**

Varying sources can be discriminated by means of bivariate polar plots techniques (Carslaw and Ropkins, 2012). Figure 7 shows how the airport activities impact the average concentrations of the factors (SVOOA, AlkOA and MO-OOA) determined via PMF. The highest concentrations of AlkOA, and MO-OOA were determined at low to moderate wind speeds (3~5 m/s) from the west and southwest ( $R = -0.35$  and  $R = -0.42$ , respectively), where terminal buildings (T1, T2, T3, T4 and TS4), two of the runways (14R/32L and 18R/36L), and a nearby hanger zone are located. Highest SVOOA contribution determined at lower wind speeds (below 2 m/s) with a correlation between them ( $R = -0.45$ ). Both SVOOA and MO-OOA are more likely to be mixed and determined by a local source at low wind speeds  $< 2$  m/s (Crilley et al., 2015; Helin et al., 2018). By contrast, the minimum significant contribution from all factors identified when the winds were originating from the northeast of the airport, with relatively higher wind speeds (above 4 m/s). Thus, based on the polar plots shown in Fig. 7 the emissions from terminal buildings and hanger zone located at the southwest of the measurement station is the major source of the total organic particle concentrations at the measurement station. The average contribution of SVOOA, AlkOA, and MO-OOA was 1.63, 0.63, and 2.35  $\mu\text{g}/\text{m}^3$ , respectively (Table S1). SVOOA and MO-OOA accounted more than 80% of the total organic mass during AVIATOR Campaign in October, 2021. The linear correlations (Pearson correlation) between (i) AlkOA with eBC and (ii) SVOOA with THC were measured under varying wind speed and directions (Fig. 8). The relative contribution of the derived factors was higher when the winds originating from southwest of the airport compared to the winds carrying air parcels to the sampling point from





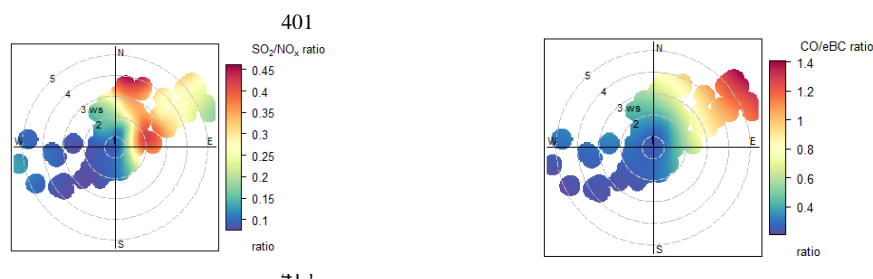
338 the northeast as discussed. However, the correlation coefficient for both varies highly ( $0.2 \leq R \leq 0.9$ ) for all  
 339 samples (from all directions) within the airport perimeter. AlkOA, for instance, has a strong linear correlation  
 340 with *e*BC (Pearson coefficient higher than 0.9) when the winds are originating from west, east or north-east as  
 341 shown in Fig. 8. This is due to the effect of runways 18L/36R and 18R/36L locations (each located on east and  
 342 west of the measurement site as shown in Fig. 1) where 90% of the aircraft take-off takes place. Both AlkOA and  
 343 *e*BC are related to jet fuel emissions. Furthermore, a significant linear correlation was measured between SVOOA  
 344 and THC when dominant winds were north easterlies (the air parcels move from runways 18L/36R to the sampling  
 345 station). THC emissions at the airports depend mainly on the jet engine thrust setting (Anderson *et al.*, 2006;  
 346 Onasch *et al.*, 2009). When the engines operate at low thrust settings (*e.g.*, during taxiing/idling), the combustion  
 347 is less efficient and a higher amount of hydrocarbons is emitted. The association between SVOOA and (THC) at  
 348 some parts of the airport could be interpreted as an indication of fresh emissions from the aircraft in service.  
 349  
 350



364  
 365  
 366  
 367  
 368  
 369  
 370  
 371  
 372  
 373  
 374  
 375  
 376  
 377  
 378  
 379  
 380  
 381  
 382  
 383  
 384  
 385  
 386  
 387  
 388  
 389  
 390  
 391  
 392  
 393  
 394  
 395  
 396  
 397  
 398  
 399  
 400

**Figure 8. A Pearson correlation analysis using bivariate polar plots (above) shows a significant positive linear correlation between AlkOA with *e*BC and SVOOA with THC mass concentrations when prevailing winds were northeast. (The location of runways 18L/36R).**

NO<sub>x</sub> emitted by aircraft can potentially affect air quality up to 2.6 km away from the airport (Carslaw *et al.*, 2006), however, there are challenges in determining an accurate contribution of the airport to local NO<sub>x</sub> concentration due to other sources (mostly mobile) of NO<sub>x</sub> in cities. In this study, the potential contribution from road traffic surrounding the airport, particularly the motorways located south and southwest of the airport, are originating from same direction where runway 14R/32L and all the terminals are also located. Therefore, NO<sub>x</sub> contribution was higher from the south and southwest of the airport (including local on-road NO<sub>x</sub>) compared to the northeast. The lowest NO<sub>x</sub> concentrations were measured under moderate wind speed conditions (above 4 m/s) (Fig. S1). This is possibly due to atmospheric mixing and plume dilution caused by advection (Carslaw *et al.*, 2006), since the ground-level source emissions are inversely proportional to wind speed. The measurements of sulphur dioxide (SO<sub>2</sub>) and carbon monoxide (CO) were available during this campaign by AENA (REDAIR) station located at the airport (Fig. S1). Aviation activities were previously reported as a significant source of SO<sub>2</sub>, while CO and NO<sub>x</sub> were mainly related to road traffic sources (Yu *et al.*, 2004). However, the bivariate polar plots presented in Fig. 9 higher SO<sub>2</sub>/NO<sub>x</sub> and CO/*e*BC ratios measured when the dominant winds originating from the northeast of the airport (with no- or little road traffic contribution). The analysis of the SO<sub>2</sub>/NO<sub>x</sub> and CO/*e*BC concentration ratios vary based on wind direction and speed in October 2021 at Madrid-Barajas Airport. The higher ambient SO<sub>2</sub>/NO<sub>x</sub> and CO/*e*BC ratios indicate the potential impact of aircraft taxiing and taking off on local ambient SO<sub>2</sub> and CO concentrations when the winds originating from northeast where the 18L/36R runways are located. SO<sub>2</sub> emissions are associated primarily with the sulphur content of the fuel, as well as emissions during aircraft activities at the airport, such as approach, taxi-idle and climb (Yang *et al.*, 2018). Black carbon (*e*BC) and carbon monoxide (CO) are mainly produced by incomplete/inefficient combustion. CO/*e*BC ratio varies significantly with the source (Bond *et al.*, 2004), which can be a sign of varying different sources in the vicinity of the airport as previously reported. The highest aircraft CO is emitted at low power engine settings (during taxiing and idling), this significantly affects the air quality within the airport as the idle and taxi phases account most of the time an aircraft spends at the airport (Stettler *et al.*, 2011; Yunos *et al.*, 2017). Higher CO/*e*BC ratios in the air parcels originating from northeast can also be attributed to the effect of aircraft activity at the runway 18L/36R located in the northeast of the measurement station. On the other hand, SO<sub>2</sub>/NO<sub>x</sub> and CO/*e*BC ratios were lower (0-0.4) when the winds were originating from southwest due to the other significant sources of NO<sub>x</sub> and *e*BC in this direction (nearby road traffic). Based on the polar plots shown in Fig. 9, an aircraft SO<sub>2</sub> and CO signal to the east and northeast is identified (different to wind-dependant NO<sub>x</sub> pattern). Further details on daily variation of meteorological parameters and trace gases for the sampling period can be found in the supplementary material (Fig. S1).



416

417

418

419

420

421

422

423

424

425

426

427

428

429

430

431

432

433

434

435

436

437

438

439

440

441

442

443

444

445

446

447

448

449

450

451

452

453

454

455

456

457

458

459

460

461

462

463

**Figure 9. Bivariate polar plots of  $\text{SO}_2/\text{NO}_x$  and  $\text{CO}/e\text{BC}$  ratios at the airport. The angular contributions of  $\text{SO}_2$  and  $\text{CO}$  is different compared to the PMF determined factors. The plots indicate that the flight activities at the east and northeast where the 18L/36R runway is located are the source of increase in  $\text{SO}_2$  and  $\text{CO}$ .**

#### 4. Conclusion

This study identified the impact of an international airport on the local air quality. As part of the AVIATOR campaign, several measurements were conducted at the Madrid-Barajas Airport, in October 2021 for monitoring the chemical composition of sub-micron particles and ambient trace gas concentrations near runway.

Total non-refractory particles were dominated by organics (more than 72% of the total). Sulphate particles were the second most abundant chemical species and accounted about 13% of the total aerosol. Based on AMS data (relative intensities of  $m/z$  71 and 85), no significant oil fraction in the organic particulate matter (PM) samples were measured. This could be either there is no oil in sub-micron particle size range or due to the method used in this study (AMS) is not able to identify lubricant oil in PM. Thus, further measurements with improved measurement technique may be required to identify oil fraction in sub-micron organic aerosol.

Trace gases were also monitored along with the particle monitoring tools. Average ambient concentrations of  $e\text{BC}$ ,  $\text{NO}_x$ ,  $\text{SO}_2$ ,  $\text{PM}_{2.5}$ ,  $\text{PM}_{10}$  at the airport during October 2021 were 1.07, 22.7, 4.10, 9.35, and 16.43 ( $\mu\text{g}/\text{m}^3$ ), respectively. By comparing angular  $\text{NO}_x$  distribution with  $\text{SO}_2/\text{NO}_x$  and  $\text{CO}/e\text{BC}$ , take-off activities at the northeast of the measurement station were identified as a potential local source of  $\text{SO}_2$  and  $\text{CO}$  in Barajas-Madrid.  $\text{NO}_x$  contribution at the sampling point was highest when the winds originating from south and southeast of the airport. There are two motorways with road traffic were located at the same direction as long as terminal buildings and southern runways in Madrid. Therefore,  $\text{NO}_x$  concentrations were more likely determined by on-road traffic compared to the aircraft activity at the sampling point. Sources of organic aerosols (as the most abundant non-refractory aerosol group) were identified via Positive Matrix Factorisation (PMF) analysis. PMF was able to discriminate three main significant sources: Semi Volatile Oxygenated Organic Aerosol (SV-OOA), Alkane Organic Aerosol (AlkOA), and More Oxidised Oxygenated Organic Aerosol (MO OOA). The sum of SV-OOA and MO OOA fractions accounting for more than 80% of the total organic mass throughout the campaign, SV-OOA had the highest relative intensity (RI) at  $m/z$  43 (which is characteristic of SVOOA), MO-OOA had a high RI at  $m/z$  28 and 44 these indicate a potential secondary aerosol fraction. Third factor, AlkOA, had high RIs at  $m/z$  43, 57 and 85 (attributed to decane previously) which is related to jet fuel vapour (Smith *et al.*, 2022).

Bivariate polar plots were used to angular PMF determined factor and ambient trace gas distributions based on wind speed and wind direction at the airport. It has been found that, the PMF determined factors had highest relative contributions when the winds originating from the west and southwest of the airport where runways 14R/32L and 18R/36L, as well as terminals T1, T2, T3, T4 and TS4, are located. Being embedded in a region with varying different sources including aircraft and airport terminal emissions, emission ratios of combustion tracers measured and angular correlation analysis based on wind direction and speed indicated that  $\text{SO}_2$  and  $\text{CO}$  emissions are potentially determined by aircraft take off activities at 18L/36R runway located along the east and northeast of the sampling point where more than 50% of the take-off activity took place in the sampling period. Further origins of the organic aerosols measured at the Madrid-Barajas were identified towards a better understanding of emissions from an international airport and provide the chemical composition of particulate matter and gaseous pollutants in the vicinity of airport.

There are two previously reported significant ways to reduce aviation emissions at airports, improving efficiency of the processes emitting air pollutants such as electrification of airport taxiway operations (Salihu *et al.*, 2021), and switching to sustainable alternative fuels where applicable. Improved ground activities at airports such as electric aircraft towing system can potentially lead up to 82 % reduction in  $\text{CO}_2$  emissions (van Baaren, 2019), while switching to SAF alone reduce Landing-takeoff cycle (LTO) emissions up to 70 % compared to fossil fuel (Schripp *et al.*, 2022). Further, SAF use for auxiliary power units (APU) also potentially reduce  $\text{NO}_x$  and  $\text{CO}_2$



464 emissions by at least 5%. Therefore, improving energy efficiency of ground activities at airports and using SAF  
465 are recommended for policymakers to improve the overall air quality at airports.

466

467 **Author contributions.** Saleh Alzahrani, Doğuşhan Kılıç, Michael Flynn, Paul I. Williams and James Allan  
468 designed the project; Saleh Alzahrani, Doğuşhan Kılıç, Michael Flynn and Paul I. Williams performed the  
469 fieldwork; Saleh Alzahrani performed the data analysis, and wrote – original draft of the article; Doğuşhan  
470 Kılıç reviewed and edited the article; Paul I. Williams and James Allan supervised, reviewed and edited the  
471 article.

472

473 **Competing interests.** At least one of the (co-) authors is a member of the editorial board of Atmospheric  
474 Chemistry and Physics.

475

#### 476 **Acknowledgments**

477

478 This project has received funding from the European Union’s Horizon 2020 research and innovation programme  
479 under Grant Agreement No 814801.

480

#### 481 **References**

482

483 Air transport statistics - Statistics Explained (europa.eu)

484

485 Amato, F., Moreno, T., Pandolfi, M., Querol, X., Alastuey, A., Delgado, A., Pedrero, M. and Cots, N., 2010.  
486 Concentrations, sources and geochemistry of airborne particulate matter at a major European airport. *Journal of*  
487 *Environmental Monitoring*, 12(4), pp.854-862.

488

489 Anderson, B.E., Beyersdorf, A.J., Hudgins, C.H., Plant, J.V., Thornhill, K.L., Winstead, E.L., Ziemba, L.D.,  
490 Howard, R., Corporan, E., Miake-Lye, R.C. and Herndon, S.C., 2011. *Alternative aviation fuel experiment*  
491 *(AAFEX)* (No. NASA/TM-2011-217059).

492

493 Anderson, B.E., Chen, G. and Blake, D.R., 2006. Hydrocarbon emissions from a modern commercial  
494 airliner. *Atmospheric Environment*, 40(19), pp.3601-3612.

495

496 Annex, I.C.A.O., 16. Environmental Protection. *Volume II Aircraft Engine Emissions*.

497

498 Bond, T.C., Streets, D.G., Yarber, K.F., Nelson, S.M., Woo, J.H. and Klimont, Z., 2004. A technology-based  
499 global inventory of black and organic carbon emissions from combustion. *Journal of Geophysical Research:*  
500 *Atmospheres*, 109(D14).

501

502 Boldo, E., Medina, S., Le Tertre, A., Hurley, F., Mücke, H.G., Ballester, F., Aguilera, I. and Daniel Eilstein on  
503 behalf of the Apehis group, 2006. Apehis: Health impact assessment of long-term exposure to PM 2.5 in 23  
504 European cities. *European journal of epidemiology*, 21, pp.449-458.

505

506 Canagaratna, M.R., Jayne, J.T., Jimenez, J.L., Allan, J.D., Alfarra, M.R., Zhang, Q., Onasch, T.B., Drewnick,  
507 F., Coe, H., Middlebrook, A. and Delia, A., 2007. Chemical and microphysical characterization of ambient  
508 aerosols with the aerodyne aerosol mass spectrometer. *Mass spectrometry reviews*, 26(2), pp.185-222.

509

510 Canonaco, F., Crippa, M., Slowik, J.G., Baltensperger, U. and Prévôt, A.S., 2013. SoFi, an IGOR-based  
511 interface for the efficient use of the generalized multilinear engine (ME-2) for the source apportionment: ME-2  
512 application to aerosol mass spectrometer data. *Atmospheric Measurement Techniques*, 6(12), pp.3649-3661.

513

514 Carslaw, D.C., Beevers, S.D., Ropkins, K. and Bell, M.C., 2006. Detecting and quantifying aircraft and other  
515 on-airport contributions to ambient nitrogen oxides in the vicinity of a large international airport. *Atmospheric*  
516 *Environment*, 40(28), pp.5424-5434.

517

518 Carslaw, D.C. and Ropkins, K., 2012. Openair—an R package for air quality data analysis. *Environmental*  
519 *Modelling & Software*, 27, pp.52-61.

520



- 521 Crilley, L.R., Bloss, W.J., Yin, J., Beddows, D.C., Harrison, R.M., Allan, J.D., Young, D.E., Flynn, M.,  
522 Williams, P., Zotter, P. and Prévôt, A.S., 2015. Sources and contributions of wood smoke during winter in  
523 London: assessing local and regional influences. *Atmospheric chemistry and physics*, 15(6), pp.3149-3171.  
524
- 525 He, R.W., Shirmohammadi, F., Gerlofs-Nijland, M.E., Sioutas, C. and Cassee, F.R., 2018. Pro-inflammatory  
526 responses to PM<sub>0.25</sub> from airport and urban traffic emissions. *Science of the total environment*, 640, pp.997-  
527 1003.  
528
- 529 Herndon, S.C., Jayne, J.T., Lobo, P., Onasch, T.B., Fleming, G., Hagen, D.E., Whitefield, P.D. and Miake-Lye,  
530 R.C., 2008. Commercial aircraft engine emissions characterization of in-use aircraft at Hartsfield-Jackson  
531 Atlanta International Airport. *Environmental science & technology*, 42(6), pp.1877-1883.  
532
- 533 Helin, A., Niemi, J.V., Virkkula, A., Pirjola, L., Teinilä, K., Backman, J., Aurela, M., Saarikoski, S., Rönkkö,  
534 T., Asmi, E. and Timonen, H., 2018. Characteristics and source apportionment of black carbon in the Helsinki  
535 metropolitan area, Finland. *Atmospheric Environment*, 190, pp.87-98.  
536
- 537 Hu, S., Fruin, S., Kozawa, K., Mara, S., Winer, A.M. and Paulson, S.E., 2009. Aircraft emission impacts in a  
538 neighborhood adjacent to a general aviation airport in Southern California. *Environmental science &*  
539 *technology*, 43(21), pp.8039-8045.  
540
- 541 Hudda, N. and Fruin, S.A., 2016. International airport impacts to air quality: size and related properties of large  
542 increases in ultrafine particle number concentrations. *Environmental science & technology*, 50(7), pp.3362-  
543 3370.  
544
- 545 Hudda, N., Gould, T., Hartin, K., Larson, T.V. and Fruin, S.A., 2014. Emissions from an international airport  
546 increase particle number concentrations 4-fold at 10 km downwind. *Environmental science &*  
547 *technology*, 48(12), pp.6628-6635.  
548
- 549 Hudda, N., Simon, M.C., Zamore, W., Brugge, D. and Durant, J.L., 2016. Aviation emissions impact ambient  
550 ultrafine particle concentrations in the greater Boston area. *Environmental science & technology*, 50(16),  
551 pp.8514-8521.  
552
- 553 Jimenez, J.L., Canagaratna, M.R., Donahue, N.M., Prevot, A.S.H., Zhang, Q., Kroll, J.H., DeCarlo, P.F., Allan,  
554 J.D., Coe, H., Ng, N.L. and Aiken, A.C., 2009. Evolution of organic aerosols in the  
555 atmosphere. *science*, 326(5959), pp.1525-1529.  
556
- 557 Jonsdottir, H.R., Delaval, M., Leni, Z., Keller, A., Brem, B.T., Siegerist, F., Schönenberger, D., Durdina, L.,  
558 Elser, M., Burtscher, H. and Liati, A., 2019. Non-volatile particle emissions from aircraft turbine engines at  
559 ground-idle induce oxidative stress in bronchial cells. *Communications biology*, 2(1), p.90.  
560
- 561 Kinsey, J.S., 2009. *Characterization of emissions from commercial aircraft engines during the Aircraft Particle*  
562 *Emissions eXperiment (APEX) 1 to 3*. Office of Research and Development, US Environmental Protection  
563 Agency.  
564
- 565 Kinsey, J.S., Dong, Y., Williams, D.C. and Logan, R., 2010. Physical characterization of the fine particle  
566 emissions from commercial aircraft engines during the Aircraft Particle Emissions eXperiment (APEX) 1–  
567 3. *Atmospheric Environment*, 44(17), pp.2147-2156.  
568
- 569 Kinsey, J.S., Hays, M.D., Dong, Y., Williams, D.C. and Logan, R., 2011. Chemical characterization of the fine  
570 particle emissions from commercial aircraft engines during the Aircraft Particle Emissions eXperiment (APEX)  
571 1 to 3. *Environmental science & technology*, 45(8), pp.  
572
- 573 Lee, D.S., Pitari, G., Grewe, V., Gierens, K., Penner, J.E., Petzold, A., Prather, M.J., Schumann, U., Bais, A.,  
574 Bernsten, T. and Iachetti, D., 2010. Transport impacts on atmosphere and climate: Aviation. *Atmospheric*  
575 *environment*, 44(37), pp.4678-4734.  
576
- 577 Li, N., Hao, M., Phalen, R.F., Hinds, W.C. and Nel, A.E., 2003. Particulate air pollutants and asthma: a  
578 paradigm for the role of oxidative stress in PM-induced adverse health effects. *Clinical immunology*, 109(3),  
579 pp.250-265.  
580



- 581 Masiol, M. and Harrison, R.M., 2014. Aircraft engine exhaust emissions and other airport-related contributions  
582 to ambient air pollution: A review. *Atmospheric Environment*, 95, pp.409-455.  
583
- 584 Mazaheri, M., Johnson, G.R. and Morawska, L., 2011. An inventory of particle and gaseous emissions from  
585 large aircraft thrust engine operations at an airport. *Atmospheric Environment*, 45(20), pp.3500-3507.  
586
- 587 NIST Mass Spectrometry Data Center. (1990). Decane, US secretary of commerce.  
588 <https://webbook.nist.gov/cgi/cbook.cgi?ID=C124185&Mask=200#Mass-Spec>.  
589
- 590 Onasch, T.B., Jayne, J.T., Herndon, S., Worsnop, D.R., Miake-Lye, R.C., Mortimer, I.P. and Anderson, B.E.,  
591 2009. Chemical properties of aircraft engine particulate exhaust emissions. *Journal of Propulsion and*  
592 *Power*, 25(5), pp.1121-1137.  
593 3415-3421.  
594
- 595 Paatero, P., 1999. The multilinear engine—a table-driven, least squares program for solving multilinear  
596 problems, including the n-way parallel factor analysis model. *Journal of Computational and Graphical*  
597 *Statistics*, 8(4), pp.854-888.  
598
- 599 Paatero, P. and Tapper, U., 1994. Positive matrix factorization: A non-negative factor model with optimal  
600 utilization of error estimates of data values. *Environmetrics*, 5(2), pp.111-126.  
601
- 602 Petzold, A. and Schönlinner, M., 2004. Multi-angle absorption photometry—a new method for the measurement  
603 of aerosol light absorption and atmospheric black carbon. *Journal of Aerosol Science*, 35(4), pp.421-441.  
604
- 605 Pope III, C.A. and Dockery, D.W., 2006. Health effects of fine particulate air pollution: lines that  
606 connect. *Journal of the air & waste management association*, 56(6), pp.709-742.  
607
- 608 Reyes-Villegas, E., Green, D.C., Priestman, M., Canonaco, F., Coe, H., Prévôt, A.S. and Allan, J.D., 2016.  
609 Organic aerosol source apportionment in London 2013 with ME-2: exploring the solution space with annual and  
610 seasonal analysis. *Atmospheric Chemistry and Physics*, 16(24), pp.15545-15559.  
611
- 612 Reyes-Villegas, E., Priestley, M., Ting, Y.C., Haslett, S., Bannan, T., Le Breton, M., Williams, P.I., Bacak, A.,  
613 Flynn, M.J., Coe, H. and Percival, C., 2018. Simultaneous aerosol mass spectrometry and chemical ionisation  
614 mass spectrometry measurements during a biomass burning event in the UK: insights into nitrate  
615 chemistry. *Atmospheric Chemistry and Physics*, 18(6), pp.4093-4111.  
616
- 617 Rissman, J., Arunachalam, S., Woody, M., West, J.J., BenDor, T. and Binkowski, F.S., 2013. A plume-in-grid  
618 approach to characterize air quality impacts of aircraft emissions at the Hartsfield–Jackson Atlanta International  
619 Airport. *Atmospheric Chemistry and Physics*, 13(18), pp.9285-9302.  
620
- 621 Salihu, A.L., Lloyd, S.M. and Akgunduz, A., 2021. Electrification of airport taxiway operations: A simulation  
622 framework for analyzing congestion and cost. *Transportation Research Part D: Transport and Environment*, 97,  
623 p.102962.  
624
- 625 Schripp, T., Anderson, B.E., Bauder, U., Rauch, B., Corbin, J.C., Smallwood, G.J., Lobo, P., Crosbie, E.C.,  
626 Shook, M.A., Miake-Lye, R.C. and Yu, Z., 2022. Aircraft engine particulate matter emissions from sustainable  
627 aviation fuels: Results from ground-based measurements during the NASA/DLR campaign ECLIF2/ND-  
628 MAX. *Fuel*, 325, p.124764.  
629
- 630 Schwarze, P.E., Øvrevik, J., Låg, M., Refsnes, M., Nafstad, P., Hetland, R.B. and Dybing, E., 2006. Particulate  
631 matter properties and health effects: consistency of epidemiological and toxicological studies. *Human &*  
632 *experimental toxicology*, 25(10), pp.559-579.  
633
- 634 Smith, L.D., Allan, J., Coe, H., Reyes-Villegas, E., Johnson, M.P., Crayford, A., Durand, E. and Williams, P.I.,  
635 2022. Examining chemical composition of gas turbine-emitted organic aerosol using positive matrix  
636 factorisation (PMF). *Journal of Aerosol Science*, 159, p.105869.  
637
- 638 Stettler, M.E.J., Eastham, S. and Barrett, S.R.H., 2011. Air quality and public health impacts of UK airports.  
639 Part I: Emissions. *Atmospheric environment*, 45(31), pp.5415-5424.  
640



- 641 Timko, M.T., Albo, S.E., Onasch, T.B., Fortner, E.C., Yu, Z., Miake-Lye, R.C., Canagaratna, M.R., Ng, N.L.  
642 and Worsnop, D.R., 2014. Composition and sources of the organic particle emissions from aircraft  
643 engines. *Aerosol Science and Technology*, 48(1), pp.61-73.  
644
- 645 Timko, M.T., Onasch, T.B., Northway, M.J., Jayne, J.T., Canagaratna, M.R., Herndon, S.C., Wood, E.C.,  
646 Miake-Lye, R.C. and Knighton, W.B., 2010. Gas turbine engine emissions—Part II: chemical properties of  
647 particulate matter.  
648
- 649 Ulbrich, I.M., Canagaratna, M.R., Zhang, Q., Worsnop, D.R. and Jimenez, J.L., 2009. Interpretation of organic  
650 components from Positive Matrix Factorization of aerosol mass spectrometric data. *Atmospheric Chemistry and  
651 Physics*, 9(9), pp.2891-2918.  
652
- 653 Ungeheuer, F., Caudillo, L., Ditas, F., Simon, M., van Pinxteren, D., Kılıç, D., Rose, D., Jacobi, S., Kürten, A.,  
654 Curtius, J. and Vogel, A.L., 2022. Nucleation of jet engine oil vapours is a large source of aviation-related  
655 ultrafine particles. *Communications Earth & Environment*, 3(1), p.319.  
656
- 657 van Baaren, E., 2019. The feasibility of a fully electric aircraft towing system.  
658
- 659
- 660 Westerdahl, D., Fruin, S.A., Fine, P.L. and Sioutas, C., 2008. The Los Angeles International Airport as a source  
661 of ultrafine particles and other pollutants to nearby communities. *Atmospheric Environment*, 42(13), pp.3143-  
662 3155.  
663
- 664 Yang, X., Cheng, S., Lang, J., Xu, R. and Lv, Z., 2018. Characterization of aircraft emissions and air quality  
665 impacts of an international airport. *Journal of environmental sciences*, 72, pp.198-207.  
666
- 667 Yim, S.H., Stettler, M.E. and Barrett, S.R., 2013. Air quality and public health impacts of UK airports. Part II:  
668 Impacts and policy assessment. *Atmospheric environment*, 67, pp.184-192.  
669
- 670 Yu, K.N., Cheung, Y.P., Cheung, T. and Henry, R.C., 2004. Identifying the impact of large urban airports on  
671 local air quality by nonparametric regression. *Atmospheric Environment*, 38(27), pp.4501-4507.  
672
- 673 Yu, Z., Herndon, S.C., Ziemba, L.D., Timko, M.T., Liscinsky, D.S., Anderson, B.E. and Miake-Lye, R.C.,  
674 2012. Identification of lubrication oil in the particulate matter emissions from engine exhaust of in-service  
675 commercial aircraft. *Environmental science & technology*, 46(17), pp.9630-9637.  
676
- 677 Yu, Z., Liscinsky, D.S., Winstead, E.L., True, B.S., Timko, M.T., Bhargava, A., Herndon, S.C., Miake-Lye,  
678 R.C. and Anderson, B.E., 2010. Characterization of lubrication oil emissions from aircraft  
679 engines. *Environmental science & technology*, 44(24), pp.9530-9534.  
680
- 681 Yu, Z., Timko, M.T., Herndon, S.C., Richard, C., Beyersdorf, A.J., Ziemba, L.D., Winstead, E.L. and Anderson,  
682 B.E., 2019. Mode-specific, semi-volatile chemical composition of particulate matter emissions from a  
683 commercial gas turbine aircraft engine. *Atmospheric Environment*, 218, p.116974.  
684
- 685 Yunos, S.N.M.M., Ghafir, M.F.A. and Wahab, A.A., 2017, April. Aircraft LTO emissions regulations and  
686 implementations at European airports. In *AIP Conference Proceedings* (Vol. 1831, No. 1).  
687
- 688 Zhang, Q., Jimenez, J.L., Canagaratna, M.R., Allan, J.D., Coe, H., Ulbrich, I., Alfarra, M.R., Takami, A.,  
689 Middlebrook, A.M., Sun, Y.L. and Dzepina, K., 2007. Ubiquity and dominance of oxygenated species in  
690 organic aerosols in anthropogenically-influenced Northern Hemisphere midlatitudes. *Geophysical research  
691 letters*, 34(13).  
692
- 693 Zhu, Y., Fanning, E., Yu, R.C., Zhang, Q. and Froines, J.R., 2011. Aircraft emissions and local air quality  
694 impacts from takeoff activities at a large International Airport. *Atmospheric Environment*, 45(36), pp.6526-  
695 6533.  
696  
697  
698  
699  
700